

Dalton Transactions

Accepted Manuscript



This is an *Accepted Manuscript*, which has been through the Royal Society of Chemistry peer review process and has been accepted for publication.

Accepted Manuscripts are published online shortly after acceptance, before technical editing, formatting and proof reading. Using this free service, authors can make their results available to the community, in citable form, before we publish the edited article. We will replace this *Accepted Manuscript* with the edited and formatted *Advance Article* as soon as it is available.

You can find more information about *Accepted Manuscripts* in the [Information for Authors](#).

Please note that technical editing may introduce minor changes to the text and/or graphics, which may alter content. The journal's standard [Terms & Conditions](#) and the [Ethical guidelines](#) still apply. In no event shall the Royal Society of Chemistry be held responsible for any errors or omissions in this *Accepted Manuscript* or any consequences arising from the use of any information it contains.



ARTICLE

Half-sandwich Rhodium and Iridium Metallamacrocycles Constructed via C-H Activation

Received 00th January 2015,
Accepted 00th January 2015

Lin Lin^a, Ying-Ying Zhang^a, Yue-Jian Lin^a and Guo-Xin Jin^{a*}

DOI: 10.1039/x0xx00000x

www.rsc.org/

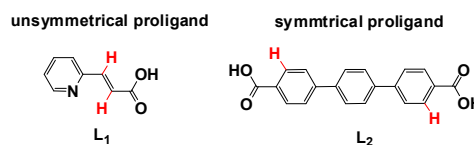
Half-sandwich Rhodium and iridium complexes with carboxylic acid ligands were combined with pyrazine, 4,4'-bipyridine (bpy) or *trans*-1,2-bis(4-pyridyl)-ethylene (bpe) to give a series of tetranuclear macrocycles. The metallamacrocycles [(Cp*Rh)₄(L₁)₂(pyrazine)₂][OTf]₂ (**1**), [(Cp*Rh)₄(L₁)₂(bpy)₂][OTf]₂ (**2**), [(Cp*Rh)₄(L₁)₂(bpe)₂][OTf]₄ (**3**) and [(Cp*Ir)₄(L₂)₂(pyrazine)₂] (**4**) (L₁ = 3-(2-pyridyl)acrylic acid, L₂ = 1,4-di(4-carboxyphenyl)benzene) were characterized by elemental analysis, NMR, IR and single-crystal X-ray analyses. Due to the different structures of the carboxylate ligands, the complexes **1a-3a, 1b-3b** and **4** were synthesized through double-site C-H activation, and complexes **1c-3c** were obtained by on-site C-H activation.

Introduction

The activation of C-H bonds is a key elementary step of organometallic reactions, and plays an important role in organic and inorganic synthesis. Whereas there have been a number of examples of C-H bond formation or cleavage promoted by transition metal complexes, either stoichiometric or catalytic, noble metal elements have been used in most cases.¹ In particular, complexes containing the Cp*Rh or Cp*Ir fragment readily undertake oxidative addition of C-H bonds.² The intramolecular C-H activation of half-sandwich metal complexes can lead to formation of metallamacrocycles, and such complexes have shown promise in several fields of chemistry.³ Thereby, the construction and modification of ligands by C-H activation and self-assembly has been developed.^{4,5} A wide range of metal-organic architectures such as metallacycles, metallaprisms, metallaboxes and metallacages have been reported based on half-sandwich metal fragments (CpM/Cp*M) as metal centers. The synthesis of these C-H activation compounds generally involves the use of simple starting materials and a relatively general procedure, and proceeds under mild conditions. For example, we normally rely on functionalization of C-H bonds of aromatic compounds (such as carboxylic acid ligands) and pyridine linkers based on half-sandwich binuclear complexes as building blocks to construct tetranuclear macrocycles. Because of this, the size and type of the carboxylic acid proligand can significantly influence the properties of the macrocycle.^{6,7}

The carboxylic acid ligands for this purpose can be divided into symmetrical and unsymmetrical groups, as shown in Scheme 1. Symmetrical carboxylate ligands with interesting structural features and technologically useful functions have been topics of intense study, and have considerable potential. Nevertheless, there have been comparatively few reports on C-H activation of unsymmetrical carboxylate ligands in the construction of metallamacrocycles until now.^{8,9}

The C-H activation of unsymmetrical carboxylate ligands has proven very useful for constructing a wide array of molecular architectures. This structure diversity also makes the half-sandwich metal macrocycles or cages suitable for various applications, including utility in host-guest chemistry, molecular recognition, electrochemical sensing and anticancer research. The intramolecular C-H bond activation of unsymmetrical carboxylate ligands can also lead to isomer complexes, and such complexes have shown promise in several fields of chemistry, particularly catalysis.¹⁰⁻¹²



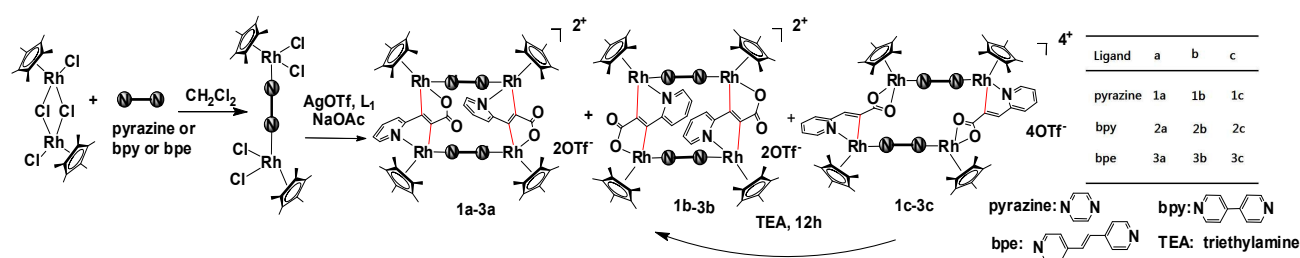
Scheme 1 Examples of symmetrical and unsymmetrical carboxylic acid proligands for C-H activation.

Over the past few years, our group has reported a range of metallamacrocycles by using C-H bond activation and Cp*Rh or Ir (Cp* = η^5 -C₅Me₅) units as building blocks for self-assembly. In general, symmetrical binuclear complexes with two available coordination sites at each metal center can be used as building blocks with bipyridine ligands to form macrocycle complexes.¹³⁻¹⁵ The rigorous exclusion of water or oxygen has become a general requirement for the C-H activation steps in this field. It is also worth

State Key Laboratory of Molecular Engineering of Polymers, Collaborative Innovation Center of Chemistry for Energy Materials, Department of Chemistry, Fudan University, Shanghai 200433, P. R. China; E-mail: gxjin@fudan.edu.cn

†Electronic Supplementary Information (ESI) available: CCDC-960936(**3c**), 960937(**1a**), 960938(**2b**), 1436256 (**1c**), 1436257 (**2c**), 1436258 (**4**), 1437166 (**1b**), 1456394(**3c**) contain the supplementary crystallographic data for this paper. See DOI: 10.1039/x0xx00000x

ARTICLE



Scheme 2. Synthesis of complexes 1 to 3.

mentioning that the quantity of sodium acetate also plays a decisive role in the formation of these C-H activation complexes.¹⁶In this work, we illustrate that unsymmetrical and symmetrical carboxylate ligands provide both high rigidity and structural stability and are not be found when ligands contain rotation axes or labile-coordinate bonds to the metal centers. Rational control of the unsymmetrical structure of carboxylic acid proligands can lead to two kinds of half-sandwich metallamacrocycles through C-H activation. One difficulty of using the proligand 3-(2-pyridyl)acrylic acid (L_1) for half-sandwich self-assembly processes is the fact that L_1 can form conformational isomers with a different relative orientation of the N-donor groups. In one case this led to double-site C-H activation involving σ -coordination to the double bond of the olefin. A number of complexes based on isomerization of L_1 were observed and unambiguously confirmed by single-crystal X-ray crystallography. Another outcome involved one-site C-H activation, coordination with the pyridyl group of 3-(2-pyridyl)acrylic acid, while the carboxylate group was found to bind through both oxygen atoms to the rhodium atom.

Inspired by these results, we also designed a symmetrical carboxylic acid as proligand through a general and efficient procedure in order to construct macrocycles via C-H bond activation. Using this proligand, C-H bond activation was induced by employing an alkaline environment. Rigid, symmetrical proligand L_2 (Scheme 1) is used to prepare metallacyclic tubular architectures by self-assembly.¹⁷In particular, macrocyclic complexes such as these may have the ability to selectively adsorb CO_2 .

Results and Discussion

As depicted in Scheme 2, we have attempted to synthesize a series of macrocycles complexes involving unsymmetrical ligands via C-H bond activation of olefinic carboxylate proligands. Therefore, the precursor complex $[Cp^*RhCl_2]_2$ was initially reacted with L (L = pyrazine, 4,4'-bipyridine or *trans*-1,2-bis(4-pyridyl)-ethylene) in dichloromethane at room temperature to produce binuclear complexes $[Cp^*RhCl_2]_2L$. Four equivalents of silver trifluoromethane sulfonate (AgOTf) were then added to the solution and the reaction was carried out in the dark for 12 hours. Sodium acetate (NaOAc) and 3-(2-pyridyl) acrylic acid were added to the solution, and the mixture was stirred for a further 10 hours. The products were washed and recrystallized from dichloromethane / diethyl ether, and

then isolated by careful selection of the crystals. Single-crystal X-ray structural analysis revealed that **1a**, **1c**, **2b**, **2c** and **3c** were formed through C-H activation. The structures of complexes were also confirmed by their 1H NMR, IR spectra, and elemental analyses. All of these metallamacrocycles were fully characterized by 1H NMR and 1H - 1H COSY. In the 1H NMR spectra, signals attributable to the 3-(2-pyridyl) acrylic acid ligand and the Cp* groups were split into two equal parts, indicating different chemical environments of this group. The existence of isomers is presumably due to the direction of the nitrogen atom from the 3-(2-pyridyl) acrylic acid ligand as shown in Scheme 2.

As shown in Scheme 2, one of the influencing factors about the C-H bond activation was the coordination site with the carboxylate ligands and metal centers. Another was the coordination model was chelating coordination or coordination with the C-H bonds to formed macrocyclic compounds. Herein, we report a method that different from previous to synthesize half-sandwich rhodium macrocycles by directed multicomponent self-assembly in which C-H activation occurs under mild conditions.

The first coordination model involves coordination of the two carboxylate ligands to rhodium atoms in a two-site coordination mode and direction. As shown in Figure 1a, each rhodium atom of **1a** is connected to one pyrazine and one pyridyl/carboxylic acid ligand; two Rh atoms are bound through C,N atoms and two Rh atoms bind through C,O atoms. The lengths of Rh4-O3, Rh1-N1, Rh3-N2, and Rh2-O1 bonds are 2.1392(2), 2.1081(2), 2.1392(2), and 2.0879(2) Å, respectively. There were disordered solvents (half of one diethyl ether molecules) which could not be restrained properly. Therefore, SQUEEZE algorithm was used to omit them. Figure 1b shows a simplified wireframe view of macrocyclic complexes **1a**. Figure 1c shows that the two neighboring layers of the complexes **1a** are linked by hydrogen bonds and the distances between the complexes **1a** are 2.7911(2), 2.7222(3) and 2.6491(2) Å. One should note that weak hydrogen bonding of this kind has frequently been observed for enantiomers based on asymmetric ligands. Through these weak hydrogen bonding interactions a one-dimensional structure was formed (Figure 1c). The one- and two-dimensional stacking structure are produced by hydrogen bonding interactions between the OTf⁻ anions and the carbon atoms of Cp* groups (Figure 1d). The structures of these complexes were confirmed by 1H NMR and elemental analysis. The features of the 1H NMR

spectra of complexes **1a**, **1b** and **1c** are similar to each other. The Cp*Rh groups [$\delta = 1.54$ ppm (**1a,1b**), and 1.57 (**1c**)] indicate that the Cp*Rh moieties of the complexes exist in similar chemical environments. The signals of complexes **1a,1b** and **1c** are different from each other due to the different configurations of the C-H activation. The existence of isomers (**1a** and **1b**) is probably due to the direction of the nitrogen atom from the 3-(2-pyridyl)acrylic acid ligand as shown in Scheme 2. The Cp*Ir group also proved to be capable of mediating the double-site C-H activations, giving **1bs** as supporting products (Figure S1). Overall, the investigation of the complexes through ^1H - ^1H COSY spectra illustrates the existence of these compounds, but it is very difficult to physically separate **1a-1b** and **1c** in solution.

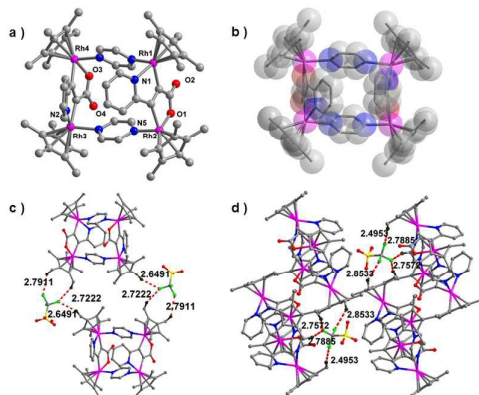


Figure 1. (a) Simplified wireframe view of complex **1a**; (b) Space-filling view of complex **1a**; (c) View showing hydrogen bonds between the OTf anions and carbon atoms of complex **1a**; (d) View showing the two-dimensional hydrogen-bonded network (gray for C, blue for N, red for O, pink for Rh, yellow for S, green for F, hark green for H).

The second coordination model is significantly different from the first, but also results in rectangular macrocycles. The carboxylate ligand undergoes C-H activation at only one position, while the two carboxylate oxygen atoms of each ligand chelate one rhodium atom (Figure 2a,b). This plasticity can be attributed to the presence of unsymmetrical ligands, which are kinetically labile and have flexible coordination geometries. The hydrogen bonds between complex **1c** are 2.7061(2) (F7-H53C), 2.6607(2) (F9-H50C), 2.5474(2) (F6-H31A), and 2.8714(2) (F5-H19) Å, respectively (Figure S2). There was one disordered dichloromethane molecule which could not be restrained properly. Therefore, SQUEEZE algorithm was used to omit it. Further analysis of the structure of complex **1c** explains why the one-dimensional channel forms. Four OTf⁻ anions were found between two neighboring layers of the macrocycles that are linked with hydrogen bonds. Among the four OTf⁻ anions, four anions were found inside the channel formed by the macrocycles with one F atom hydrogen bonding to a hydrogen atom of the Cp* group, the distances being 2.6565(2) (F4-H53C), 2.7347(2) (F3-H31D), 2.7401(2) (F9-H32F), and 2.7716(2) (F10-H34A) Å (Figure S2).

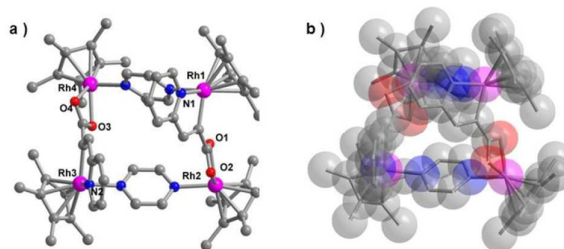


Figure 2. (a) Simplified wireframe view of complex **1c**; (b) Space-filling view of complex **1c** (gray for C, blue for N, red for O, pink for Rh).

In order to test whether the singly-activated ligands of complex **1c** could be induced to undergo a second C-H activation, we investigated the reaction of **1c** under basic conditions. Mixing a dichloromethane (10 mL) solution of C-H-activated complexes **1a-1c** (0.1 mmol) with triethylamine (0.2 mL) for 12 h resulted in the formation of complexes **1a,b** which contain double-site C-H activated ligands. The ^1H NMR spectra of complexes **1a,b** showed a single set of signals for the 3-(2-pyridyl)acrylic acid ligands and pyrazine ligands, in accordance with a two-site C-H activation structure (Figure S8). As a consequence, the interconversion between the two types of C-H bond activation does not proceed in both directions: the one-site activated complex (**1c**) can be converted to two-site complexes (**1a,b**) but not vice versa.

A similar tetranuclear structure was confirmed for complex **2b** by single-crystal X-ray diffraction study. This assumption was also confirmed by ^1H - ^1H COSY spectra analysis of the complexes **2a-2c** (Figure S10). Figure 3a shows that the two 4,4'-bipyridine ligands are orthogonal to the planes made by the two rhodium atoms and the pyridyl/carboxylate ligands. The tetranuclear structure **2b** shows a rectangle with dimensions of 4.8195(3) and 11.3083(6) Å for the Rh1B-Rh2A and Rh1A-Rh2A distances. There were disordered solvents (three water and one methanol molecules) which could not be restrained properly. Therefore, SQUEEZE algorithm was used to omit them. The two OTf⁻ anions and the Cp* groups lead to the one- and two-dimensional hydrogen bonded networks as previously described (Figure S3).

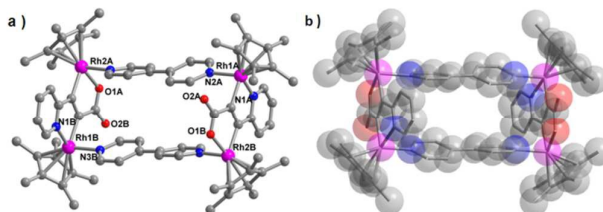


Figure 3. (a) Simplified wireframe view of complex **2b**; (b) Space-filling view of complex **2b** (gray for C, blue for N, red for O, pink for Rh).

The structure of complex **2c** is shown in Figure 4a, the distances between the pyridyl/carboxylate-bridged and bpy-bridged Rh atoms are 5.470 Å and 11.277 Å, respectively. The two bpy groups were found to be nearly perpendicular to the 3-(2-pyridyl)acrylic acid ligands. The average Rh2B-O2B (2.1526(3) Å) and Rh2B-O1B (2.1561(3) Å) bond lengths are similar to those found for the double-site C-H activation complex **2b** (Rh2A-O1A = 2.0918(1) Å; Rh1B-N1B = 2.0993(1) Å). There were disordered solvents (four methanol and three water molecules) which could not be restrained properly. Therefore, SQUEEZE algorithm was used to omit them. The two-dimensional network of complex **2c** in the

ARTICLE

Dalton Transactions

crystal is shown in Figure S4. There are some weak hydrogen bonding interactions between the F atoms of the OTf⁻ anions and the hydrogen atoms of the Cp* groups. Attempts to crystallographically characterize complex **2a** were not successful due to poor quality data and large numbers of solvent molecules.

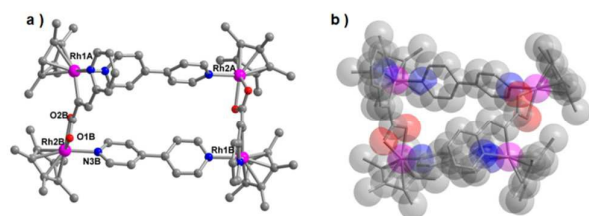


Figure 4. (a) Simplified wireframe view of complex **2c**; (b) Space-filling view of complex **2c** (gray for C, blue for N, red for O, pink for Rh).

As shown in Figure 5a, complex **3c** has an analogous connectivity to **1c** and **2c**; however, its rectangular structure is significantly distorted. The two bridging bpe ligands are also slightly bent. As a consequence, the distance between the two parallel ethylene C atoms was 5.4849(7) Å, whereas the N atoms, being 5.9950(8) and 5.4950(7) Å apart, were nearly parallel to each other. There were disordered solvents (one dichloromethane and one diethyl ether molecules) which could not be restrained properly. Therefore, SQUEEZE algorithm was used to omit them. We also obtained an analogous iridium complex **3cs** shown in Figure S15. From the Figure 5b, it can be seen that the bpe ligands are not strictly parallel, which may be unfavorable for [2+2] photocycloaddition. When single crystals or a powdered crystalline sample of complex **3c** was subjected to UV irradiation using an Hg lamp for a period of approximately 25 h, no dimerization reaction was observed, as evident by ¹H NMR spectroscopy. To gain further insight into this complex **3c**, ¹H NMR experiments were carried out in CD₃OD to investigate the ability and selectivity of the metallarectangle to host small organic molecules. However, no obvious changes for observed. Figure S5 shows four OTf⁻ anions connected to the Cp* groups of two neighboring macrocycles through their F atoms, with hydrogen bonds distances from 2.689 to 2.821 Å. The two-dimensional extended structure of complex **3c** in the crystal is shown in Figure S5.

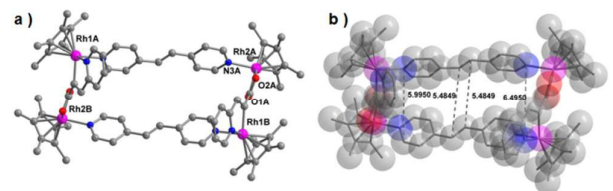
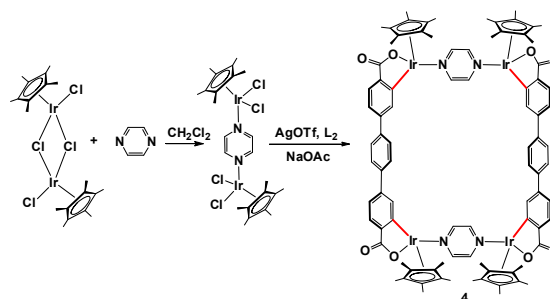


Figure 5. (a) Simplified wireframe view of complex **3c**; (b) Space-filling view of complex **3c** (gray for C, blue for N, red for O, pink for Rh).

These results with unsymmetrical ligands prompted us to explore the supramolecular coordination chemistry of symmetrical ligands using iridium complexes suitable for C-H activation. Therefore, we attempted to obtain a macrocycle by using symmetrical ligands based on 1,4-di(4-carboxyphenyl)benzene. As indicated in Scheme 3, the macrocycle **4** was obtained by reaction of [Cp*IrCl₂]₂ with pyrazine. Similarly, a tetranuclear complex was obtained by reaction of binuclear complexes with 1,4-di(4-

carboxyphenyl)-benzene in the presence of sodium acetate. This may indicate that the C-H activation and metallacycle formation is cooperative, and that the symmetry and stability of the metallacycle partly restriction the self-assembly formation. And the size and steric hindrance of the C-H bond is one of the crucial factors to affect the interaction between the four Cp*Ir units and symmetric ligands.



Scheme 3. Synthesis of metallacycle **4**.

The structure of complex **4** shows two pyrazine ligands linked by two 1,4-di(4-carboxyphenyl)benzene units to form a M₄L₂ macrocycle (Figure 6a). Figure 6b shows that the most salient feature of **4is** that the 1,4-di(4-carboxyphenyl)benzene unit binds as a bidentate ligand at two positions, via activation of two C-H bonds. The Ir1A-O1A and Ir1B-O1B distances are both 2.0115(2) Å. There were disordered solvent molecules (half of a dichloromethane molecule) which could not be restrained properly. Therefore, SQUEEZE algorithm was used to omit it. The high symmetry and stability of the structure is presumably due to the formation of five-membered chelate rings at each Ir center. The complex **4** adopts a rectangular structure with Ir1A-Ir1B distances of 12.5286(19) Å. The Ir1-Ir3 distance is 6.9285(11)Å, while the Ir1A-N1A and Ir1D-N1D distances are both 2.0673(3) Å. Interestingly, three-dimensional molecular tunnels are obvious from viewing the crystal packing (Figure 6d).

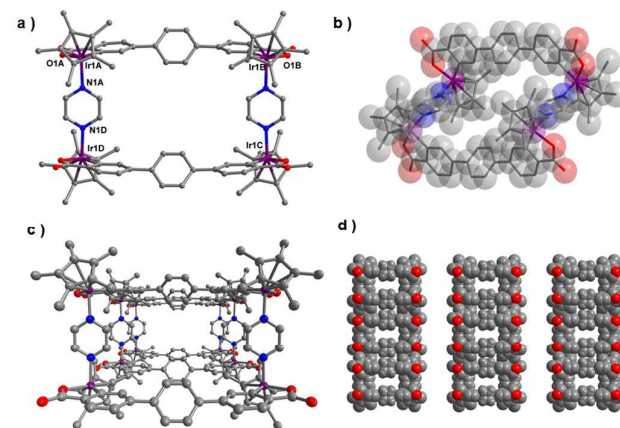


Figure 6. (a) Simplified wireframe view of complex **4**; (b) Space-filling view of complex **4**; (c) Crystal-stacking structure of complex **4**; (d) Channel-stacking architecture of complex **4** (gray for C, blue for N, red for O, purple for Ir).

Furthermore, the possibility of adsorption and separation of CO₂ using porous, solid adsorbents has received much attention during the past decade as an alternative for amine-based absorption-desorption processes. The group of Zhang reported that purely

organic cages with N–H groups show ideal selectivity of CO₂/N₂.¹⁸ In this work, single-component gas sorption experiments were carried out on CO₂ and N₂ up to 1 atm at 77.35K (Fig. S12). We observed that almost no adsorption of nitrogen and the highest selectivity ratio CO₂ of the unsymmetric ligand complex **3a,b** was shown to be 4.05cm³/g at 77.35 K and 0.87atm. The symmetric ligand complex **4** can improve the adsorbed amounts of CO₂ (4.62cm³/g at 77.35 K and 0.96atm) which corresponds to the defects, such as mesopore formation as a result of fragmentary framework collapse during the transformation. The influencing factors on adsorptive gas separation include the molecular sieving effect, the thermo-dynamic equilibrium effect, and the kinetic effect which have contribution to the highly selective capture of CO₂ rather than N₂.

Experimental Section

General procedures: The syntheses of the complexes were carried out under an atmosphere of nitrogen using standard Schlenk techniques. Dichloromethane and methanol were purified by standard methods prior to use. The starting materials [Cp*RhCl₂]₂ and [Cp*IrCl₂]₂ were prepared according to literature procedures.²⁰ Other chemicals were obtained commercially and used without further purification. Elemental analyses were performed on an Elementar III Vario EI analyzer. ¹H NMR spectra (400 MHz) were recorded on a Bruker DMX-500 Spectrometer in CD₃OD (δ3.31) or CDCl₃ (δ7.26) solutions. IR spectra were measured on a Nicolet Avatar-360 spectrometer.

Syntheses and Characterizations.

Preparation of 1a-1c. A solution of [Cp*RhCl₂]₂ (31.0 mg, 0.05mmol) and pyrazine (4 mg, 0.05 mmol) in dichloromethane (10 mL) was stirred for 4 h at room temperature. AgOTf (0.2 mmol) was added to the solution and the reaction was stirred in the dark for 12 h. Subsequently, 3-(2-pyridyl)acrylic acid (7.5 mg, 0.05 mmol) was added to the solution along with sodium acetate (41 mg, 0.5mmol), and vigorous stirring was continued for 4 hat room temperature. The products were crystallized from dichloromethane / diethyl ether to give complexes **1a-1c**. (Yield: **1a-1b**: 42.6 mg, 66.2%, red block crystals; **1c**: 4.8 mg, 7.4%, orange block crystals). *Data for complex 1a-1c: Elemental Analysis: 1a,b:* Anal. Calcd for C₆₆H₇₆N₆Rh₄F₆O₁₀S₂: C 46.55, H 4.50, N 4.93. Found: C46.03, H 4.26, N 4.61; **1c:** Anal. Calcd for C₆₆H₇₈N₆Rh₄F₁₂O₁₆S₄: C 40.05, H 3.97, N 4.25. Found: C 40.53, H 4.20, N 4.58. *Data for complexes 1a-1c: ¹H NMR: 1a,b ¹H NMR* (400 MHz, CD₃OD, ppm): δ = 8.84-8.70 (d, 2H, Py-H), 8.47-8.43 (d, 4H, pyrazine-H), 8.32-8.27 (d, 4H, pyrazine-H), 7.87-7.83 (t, 2H, Py-H), 7.42-7.35 (t, 2H, Py-H), 7.32-7.26 (t, 2H, Py-H), 1.63-1.54 (m, 60H, Cp*-H); **1c ¹H NMR** (400 MHz, CD₃OD, ppm): δ = 9.04-9.01 (d, 2H, Py-H), 8.97-8.90 (d, 2H, Py-H), 8.71-8.62 (d, 2H, Py-H), 8.40-8.37 (d, 4H, pyrazine-H), 8.17-8.16 (t, 2H, Py-H), 8.04-8.02 (d, 4H, pyrazine-H), 7.54-7.50 (t, 2H, CH=C), 1.65-1.57 (d, 60H, Cp*-H). *Data for complex 1a-1c IR* (KBr disk): 3100, 2963, 2914, 1602, 1573, 1557, 1538, 1455, 1396, 1260, 1223, 1156, 1105, 1030, 801, 754, 637, 572, 517 cm⁻¹.

Preparation of 2a-2c. [Cp*RhCl₂]₂ (31.0 mg, 0.05mmol) and 4,4'-bipyridine (8 mg, 0.05 mmol) were added to a solution of the

dichloromethane (10 mL). The following operation was same as **1a-1c**. Subsequently, the products were crystallized from dichloromethane / diethyl ether to give complexes **2a-2c**. (Yield: **2a,b**: 39.12 mg, 56.8%, orange block crystals; **2c**: 12.5 mg, 18.2%, yellow block crystals). *Data for complex 2a-2c: Elemental Analysis: 2a,b:* Anal. Calcd for C₇₈H₈₈N₆Rh₄F₆O₁₀S₂: C 50.39, H 4.77, N 4.52. Found: C 50.82, H 4.98, N 4.84; **2c:** Anal. Calcd for C₇₈H₉₀N₆Rh₄F₁₂O₁₆S₄: C 43.87, H 4.25, N 3.94. Found: C 43.42, H 4.02, N 3.63. *Data for complex 2a-2c: ¹H NMR: 2a,b ¹H NMR* (400 MHz, CD₃OD, ppm): δ = 9.01-8.96 (d, 2H, Py-H), 8.39-8.35 (d, 2H, Py-H), 8.21-8.17 (d, 2H, Py-H), 8.01-7.95 (t, 2H, Py-H), 7.84-7.70 (t, 18H, bpy-H), 7.29-7.21 (t, 18H, bpy-H), 1.63-1.62 (m, 60H, Cp*-H); **2c ¹H NMR** (400 MHz, CD₃OD, ppm): δ = 9.08-9.02 (d, 2H, Py-H), 8.44-8.40 (t, 2H, Py-H), 8.28-8.23 (t, 2H, Py-H), 8.09-7.96 (t, 8H, bpy-H), 7.44-7.30 (t, 8H, bpy-H), 7.20-7.17 (s, 2H, CH=C), 1.67-1.63 (d, 60H, Cp*-H). *Data for complex 2a-2c: IR* (KBr disk): 3094, 2975, 2919, 1619, 1572, 1500, 1460, 1438, 1379, 1260, 1218, 1161, 1065, 842, 791, 756, 639, 580, 559, 516cm⁻¹.

Preparation of 3a-3c. 4,4'-bpe (9 mg, 0.05 mmol) was stirred with [Cp*RhCl₂]₂ (31 mg, 0.05 mmol) in dry dichloromethane (10 mL) for 4 h at room temperature. The solution was then worked up according to the synthetic method of complexes **1a-1c**. Finally, the products were crystallized from dichloromethane / diethyl ether to give complexes **3a-3c**. (Yield: **3a,b**: 38.2 mg, 54.7%, orange block crystals; **3c**: 11.8 mg, 16.9%, yellow block crystals). *Data for complex 3a-3c: Elemental Analysis: 3a,b:* Anal. Calcd for C₈₂H₉₂N₆Rh₄F₆O₁₀S₂: C 51.53, H 4.85, N 4.40. Found: C 51.91, H 5.14, N 4.65; **3c:** Anal. Calcd for C₈₂H₉₄N₆Rh₄F₁₂O₁₆S₄: C 45.02, H 4.33, N 3.84. Found: C 45.62, H 4.65, N 4.08. *Data for complex 3a-3c ¹H NMR: 3a,b ¹H NMR* (400 MHz, CD₃OD, ppm): δ = 8.97-8.91 (d, 2H, Py-H), 8.57-8.44 (d, 2H, Py-H), 8.25-8.20 (d, 2H, Py-H), 8.12-8.07 (d, 4H, Py-H), 7.88-7.70 (t, 2H, Py-H), 7.23-7.02 (m, 16H, bpe-H), 1.67-1.63 (m, 60H, Cp*-H); **3c ¹H NMR** (400 MHz, CD₃OD, ppm): δ = 9.07-8.98 (d, 2H, Py-H), 8.76-8.71 (d, 2H, Py-H), 8.31-8.24 (d, 2H, Py-H), 8.18-8.14 (t, 2H, Py-H), 8.03-7.89 (t, 8H, bpe-H), 7.88-7.70 (t, 8H, bpe-H), 7.41-7.32 (d, 4H, ethylene-H), 7.31-7.26 (d, 2H, CH=C), 1.63-1.61 (d, 60H, Cp*-H). *Data for complex 3a-3c: IR* (KBr disk): 3100, 2965, 2916, 1609, 1568, 1455, 1413, 1383, 1261, 1223, 1157, 1071, 1030, 821, 756, 638, 573, 517 cm⁻¹.

Preparation of 4. A solution of [Cp*IrCl₂]₂ (80.0 mg, 0.1 mmol) and pyrazine (8 mg, 0.1mmol) in dichloromethane (10 mL) was stirred for 4 h at room temperature. AgOTf (0.4 mmol) was added to the solution and the reaction was carried out in the dark for 12 h. 1,4-di(4-carboxyphenyl)benzene (31.8 mg, 0.1mmol) was then added to the solution along with sodium acetate (82 mg, 1.0mmol), vigorous stirring was continued for 4 h. The solution was concentrated to give a dark red solid, which was washed with diethyl ether and dried under vacuum. Finally, the products were crystallized from dichloromethane / diethyl ether to give complex **4** (Yield: 54.2 mg, 78.1%, orange block crystals). *Data for complex 4: Elemental Analysis:* Anal. Calcd for C₈₈H₆₈Ir₄N₄O₈: C 50.85, H 3.30, N 2.70. Found: C 50.31, H 3.11, N 2.43. ¹H NMR (400 MHz, CD₃OD, ppm): δ = 8.81-8.62 (d, 8H, benzene-H), 7.90-7.75 (d, 8H, benzene-H), 7.48-7.02 (t, 8H, benzene-H), 5.88-5.04 (d, 4H, benzene-H), 1.64-1.42 (d, 60H, Cp*-H). *Data for complex 4 IR* (KBr disk): 3510, 1607,

ARTICLE

Dalton Transactions

1473, 1416, 1393, 1223, 1175, 1073, 1030, 821, 791, 779, 756, 638, 573, 517, 465 cm⁻¹.

Single-Crystal X-ray Structure Determination. All the determinations of unit cell data was performed with graphite-monochromated MoK α radiation ($\lambda = 0.71073 \text{ \AA}$) for complexes **1** to **4**. All the data were collected at different temperature (**1a**, **2b**, **2c**, **3c**, **4**, **3cs**: 173K; **1c**: 193K; **1bs**: 293K) using the ω scan technique. These structures were solved by direct methods, using Fourier techniques, and refined on F² by a full-matrix least-squares method. All the calculations were carried out with the SHELXTL program.²¹ A summary of the crystallographic data and selected experimental information are given in Table1. CCDC-960936(**3c**), 960937(**1a**), 960938(**2b**), 1436256 (**1c**), 1436257 (**2c**), 1436258 (**4**), 1437166 (**1bs**), 1456394(**3cs**) contain the supplementary crystallographic data for this paper. These data can be obtained free of charge from

TheCambridge Crystallographic Data Centre via www.ccdc.cam.ac.uk/data_request/cif.

Conclusions

In summary, we have employed C-H bond activation to construct half-sandwich iridium and rhodium macrocycles utilizing symmetrical and unsymmetrical carboxylate ligands. As expected, the formation of the metallamacrocycle complexes was achieved through C-H activation with **L**₁. The macrocyclecomplexes with more flexible unsymmetrical carboxylate ligands lead to the existence of isomers during macrocycle construction. In solution, complex**1c** can transform into complexes **1a-1b**, as determined by ¹H NMR and ¹H-¹H COSY spectra in CD₃OD-d₄ with triethylamine.

Table1. Crystallographic data for complexes **1a**, **1c**, **2b**, **2c**, **3c**, **4**.

Complex	1a	1c	2b	2c	3c	4
empirical formula	C ₆₉ H ₈₃ F ₆ N ₆ O _{11.5} Rh ₂ S ₂	C ₆₇ H ₈₄ F ₁₂ N ₆ O ₁₆ Rh ₂ S ₄	C ₆₂ H ₁₁₂ F ₆ N ₆ O ₂₀ Rh ₂ S ₂	C ₈₈ H ₁₃₀ F ₁₂ N ₆ O ₂₆ Rh ₂ S ₄	C ₁₁₄ H ₁₂₀ N ₆ Rh ₂ F ₁₂ O ₁₉ S ₄	C ₉₂ H ₈₀ Ir ₂ N ₆ O ₈
crystal size [mm ³]	0.11×0.03×0.02	0.18×0.10×0.10	0.18×0.08×0.07	0.45×0.20×0.10	0.08×0.06×0.06	0.21×0.130×0.08
space group	P 21/n	P 21/n	C 2/c	C 2/c	C 2/c	F m mm
a [Å]	16.5853(17)	22.8010(19)	35.819(2)	29.337(5)	20.953(4)	10.157(16)
b [Å]	14.0474(14)	12.6790(11)	14.2489(9)	14.113(2)	15.154(3)	25.995 (4)
c [Å]	32.107(3)	32.042(3)	19.1425(13)	14.318(2)	35.765(7)	53.545(8)
α [°]	90	90	90	90	90	90
β [°]	102.123(2)	97.4570(10) ^a	109.8460(10)	112.280(3)	101.596(3)	90
γ [°]	90	90	90	90	90	90
Volume	7313.4(13)	9184.7(13)	9189.7(10)	5485.3(16)	11124(4)	14137(4)
Z	4	4	4	2	4	4
F(000)	3596	4536	4288	2584	5512	4736
max./min. transmission	0.745/0.575	0.746/0.635	0.745/0.675	0.745/0.617	0.745 /0.633	0.746/0.374
data/restraints/parameter	12848/173 / 928	21129/168/1107	9331 / 44 / 566	11168 / 55 / 555	9739 / 74 / 656	4334 / 25 / 219
goodness of fit	1.061	1.025	1.095	0.964	1.092	1.048
Reflections collected/	43045	66884	30406	18510	32280	25216
Independent reflections	12848	21129	9331	11168	9739	4334
R1/wR2 [I > 2 σ (I)] [a]	0.0807/ 0.2049	0.0557/0.1378	0.0544/0.1488	0.0519/0.1324	0.1272/0.3125	0.0516/0.1500
R1/wR2 (all data) [a]	0.1204/0.2275	0.0829/0.1500	0.0653/0.1565	0.0719/0.1424	0.1489/0.3256	0.0659/0.1567
Crystal system	Monoclinic	Monoclinic	Monoclinic	Monoclinic	Monoclinic	Orthorhombic

[a] R1 = $\sum ||F_o| - |F_c||$ (based on reflections with $F_o > 2\sigma(F)$); wR2 = $[\sum (w(F_o - F_c)^2)]^{1/2}$; w = $1/[\sigma^2(F_o) + (0.095P)^2]$; P = $[\max(F_o, 0) + 2F_c]/3$ (also with $F_o > 2\sigma(F)$)

Furthermore, nano-sized channels self-assemble by hydrogen bond interactions in complexes **1-3**. Therefore, varying the structural characteristics of these half-sandwich complexes employed in the self-assembly process may give rise to new functional properties. Finally, the ligand **L**₂ can provide both strong M-C bonds via C-H activation, and a geometrically convenient route for intramolecular channel stacking. The results of CO₂ adsorption and separation experiments indicate that complexes constructed using symmetrical carboxylic acid ligands may be useful in the controllable release of CO₂ molecules.

Acknowledgements

This work was supported by the National Science Foundation of China (21531002, 21374019), the Program for Changjiang Scholars and Innovative Research Team in University (IRT1117), the

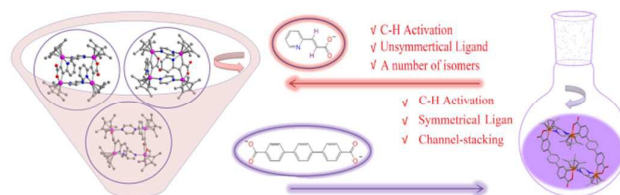
National Basic Research Program of China (2015CB856600) and the Shanghai Science Technology Committee (13JC1400600, 13DZ2275200).

References

- 1 a) T. Naota, H. Takaya, S.-I. Murahashi, *Chem. Rev.* 1998, **98**, 2599; b) C. Jia, T. Kitamura, Y. Fujiwara, *Acc. Chem. Res.* 2001, **34**, 633; c) M.-D. Su, S.-Y. Chu, *Chem. Eur. J.* 1999, **5**, 198; d) L. Ackermann, *Angew. Chem. Int. Ed.* 2011, **50**, 3842; e) C. B. Pamplin, P. Legzdins, *Acc. Chem. Res.* 2003, **36**, 223; f) R. Giri, B.-F. Shi, K. M. Engle, N. Mangel, J.-Q. Yu, *Chem. Soc. Rev.* 2009, **38**, 3242.
- 2 a) V. Ritleng, C. Sirlin, M. Pfeffer, *Chem. Rev.* 2002, **102**, 1731; b) F. Kakiuchi, S. Murai, *Acc. Chem. Res.* 2002, **35**, 826; c) A. S. Dudnik, V. Gevorgyan, *Angew. Chem. Int.*

- Ed. 2010, **49**, 2096; d) G. Dyker, *Angew. Chem., Int. Ed.* 1999, **38**, 1698.
- 3 a) F. Schmitt, J. Freudenreich, N. P. E. Barry, L. Juillerat-Jeanneret, Georg Suess-Fink, B. Therrien, *J. Am. Chem. Soc.* 2012, **134**, 754; b) L. D. David, M. A. -D. Steven, A. -D. Omar, A. M. Stuart, P. Manuel, *J. Am. Chem. Soc.* 2006, **128**, 4210; c) K. Parthasarathy, C. Bolm, *Chem. Eur. J.* 2014, **20**, 4896; d) D. Alberico, M. E. Scott, M. Lautens, *Chem. Rev.* 2007, **107**, 174; e) C. Bolm, J. Legros, J. L. Paih, L. Zani, *Chem. Rev.* 2004, **104**, 6217.
- 4 a) C. R. Turlington, J. Morris, P. S. White, W. W. Brennessel, W. D. Jones, M. Brookhart, J. L. Templeton, *Organometallics* 2014, **33**, 4442; b) T. M. Figg, S. Park, J. Park, S. Chang, D. G. Musaev, *Organometallics* 2014, **33**, 4076; c) L. Liu, Y.-L. Wu, T. Wang, X. Gao, J. Zhu, Y.-F. Zhao, *J. Org. Chem.* 2014, **79**, 5074; d) J. Li, W. Hu, Y.-M. Peng, Y.-M. Zhang, J. D. Li, W.-X. Zheng, *Organometallics* 2014, **33**, 2150; e) J. S. Cannon, L.-F. Zou, P. Liu, Y. Lan, D. I. O'Leary, K. N. Houk, R. H. Grubbs, *J. Am. Chem. Soc.* 2014, **136**, 6733; f) C. He, S. Guo, J. Ke, J. Hao, H. Xu, H.-Y. Chen, A.-W. Lei, *J. Am. Chem. Soc.* 2012, **134**, 5766.
- 5 a) T. Nishikata, A. R. Abela, B. H. Lipshutz, *Angew. Chem. Int. Ed.* 2010, **49**, 781; b) J. Ammer, C. Nolte, K. Karaghiosoff, S. Thallmair, P. Mayer, R. D. Vivie-Riedle, H. Mayr, *Chem. Eur. J.* 2013, **19**, 14612; c) L. Ackermann, R. Vicente, A. R. Kapdi, *Angew. Chem. Int. Ed.* 2009, **48**, 9792; d) P. Thansandote, M. Lautens, *Chem. Eur. J.* 2009, **15**, 5874; e) O. Daugulis, H.-Q. Do, D. Shabashov, *Acc. Chem. Res.* 2009, **42**, 1074.
- 6 a) S.-Y. Yang, X.-L. Deng, R.-F. Jin, P. Naumov, M. K. Panda, R.-B. Huang, L.-S. Zheng, B. K. Teo, *J. Am. Chem. Soc.* 2014, **136**, 558; b) Y. Ohki, T. Hatanaka, K. Tatsumi, *J. Am. Chem. Soc.* 2008, **130**, 17174; c) S. Leininger, B. Olenyuk, P. J. Stang, *Chem. Rev.* 2000, **100**, 853; d) Y. Yamauchi, M. Yoshizawa, M. Fujita, *J. Am. Chem. Soc.* 2008, **130**, 5832; e) K. Benan, M. Sebastian, R.-J. Thomas, S. Rosario, K. Severin, *Inorg. Chem.* 2012, **51**, 5795; f) C.-Z. Shao, M. Stolte, F. Würthner, *Angew. Chem. Int. Ed.* 2013, **52**, 10463.
- 7 a) S.-L. Huang, Y.-J. Lin, T. S. Andy Hor, G.-X. Jin, *J. Am. Chem. Soc.* 2013, **135**, 8125; b) Y.-B. Xie, H. Yang, Z. Y.-U. Wang, Y. Y. Liu, H.-C. Zhou, J.-R. Li, *Chem. Commun.* 2014, **50**, 563.
- 8 a) A. H. Janowicz, R. G. Bergman, *J. Am. Chem. Soc.* 1983, **105**, 3929; b) R. A. Periana, R. G. Bergman, *J. Am. Chem. Soc.* 1984, **106**, 7272; c) P. O. Stoutland, R. G. Bergman, *J. Am. Chem. Soc.* 1985, **107**, 4581.
- 9 a) Y.-F. Han, G.-X. Jin, *Chem. Asian J.* 2011, **6**, 1348; b) Y.-F. Han, H. Li, Z. -F. Zheng, G.-X. Jin, *Chem. Asian J.* 2012, **7**, 1243.
- 10 a) L.-L. Zhang, L.-H. Li, Y.-Q. Wang, Y.-F. Yang, X.-Y. Liu, Y.-M. Liang, *Organometallics* 2014, **33**, 1905; b) R. Chakrabarty, P. S. Mukherjee, P. J. Stang, *Chem. Rev.* 2011, **111**, 6810; c) Y.-F. Han, G.-X. Jin, *Acc. Chem. Res.* 2014, **47**, 3571; d) D. Munz, T. Strassner, *Inorg. Chem.* 2015, **54**, 5043; e) Y.-F. Han, Y.-J. Lin, T. S. Andy Hor, G.-X. Jin, *Organometallics* 2012, **31**, 995.
- 11 a) D. Fiedler, D. H. Leung, R. G. Bergman, K. N. Raymond, *Acc. Chem. Res.* 2005, **38**, 351; b) I. Fabre, N. V. Wolff, G. L. Duc, E. F. Flegeau, C. Bruneau, P. H. Dixneuf, A. Jutand, *Chem. Eur. J.* 2013, **19**, 7595.
- 12 D. Y.-K. Chen, S. W. Youn, *Chem. Eur. J.* 2012, **18**, 9452.
- 13 a) W.-B. Yu, Y.-F. Han, Y.-J. Lin, G.-X. Jin, *Organometallics* 2011, **30**, 3090; b) W.-B. Yu, Y.-F. Han, Y.-J. Lin, G.-X. Jin, *Chem. Eur. J.* 2011, **17**, 1863; c) W.-B. Yu, Y.-F. Han, Y.-J. Lin, G.-X. Jin, *Organometallics* 2010, **29**, 2827; d) W.-B. Yu, Y.-J. Lin, G.-X. Jin, *Organometallics* 2010, **30**, 3905.
- 14 a) L. Zhang, H. Li, L.-H. Weng, G.-X. Jin, *Organometallics* 2014, **33**, 587; b) H. Li, Y.-F. Han, G.-X. Jin, *Dalton Trans.* 2011, **40**, 4982; c) S. Shanmugaraju, A. K. Bar, Pa. S. Mukherjee, *Inorg. Chem.* 2010, **49**, 10235; d) S. Mukherjee, P. S. Mukherjee, *Chem. Commun.*, 2014, **50**, 2239; e) P. S. Mukherjee, N. Das, Y. K. Kryschenko, A. M. Arif, P. J. Stang, *J. Am. Chem. Soc.* 2004, **126**, 2464; f) N. Das, P. S. Mukherjee, A. M. Arif, P. J. Stang, *J. Am. Chem. Soc.* 2003, **125**, 13950.
- 15 a) L. Johansson, M. Tilset, *J. Am. Chem. Soc.* 2001, **123**, 739; b) L. Johansson, O. B. Ryan, C. Rømming, M. Tilset, *J. Am. Chem. Soc.* 2001, **123**, 6579; c) H. Grounds, J. C. Anderson, B. Hayter, A. J. Blake, *Organometallics* 2009, **28**, 5289.
- 16 V. Vajpayee, Y. H. Song, T. R. Cook, H. Kim, Y. Lee, P. J. Stang, K. -W. Chi, *J. Am. Chem. Soc.* 2011, **133**, 19646.
- 17 M. T. Whited, R. H. Grubbs, *Acc. Chem. Res.* 2009, **42**, 1607-1616.
- 18 a) Y.-H. Jin, B. A. Voss, A. Jin, H. Long, R. D. Noble, W. Zhang, *J. Am. Chem. Soc.* 2011, **133**, 6650; b) S.-L. Huang, G.-X. Jin, *Cryst. Eng. Comm.* 2011, **13**, 6013; c) B.-B. Tu, Q.-Q. Pang, D. F. Wu, Y. N. Song, L. H. Weng, Q. W. Li, *J. Am. Chem. Soc.* 2014, **136**, 14465.
- 19 H. Piotrowski, K. Polborn, G. Hilt, K. Severin, *J. Am. Chem. Soc.* 2001, **123**, 2699.
- 20 C. White, A. Yates, P. M. Maitlis, *Inorg. Synth.* 1992, **29**, 228.
- 21 a) SHELXS-97: G. M. Sheldrick, *Acta Crystallogr. Sect. A* 1990, **46**, 467; b) SHELXS-97: G. M. Sheldrick, *Acta Crystallogr. Sect. A* 2008, **64**, 112.

Toc Graphic



Text:

One- or two-site C-H activation of unsymmetrical and symmetrical proligands is employed to prepare a range of rectangular metallomacrocycles with a range of isomers. The CO₂ adsorption of the complexes was studied, and the symmetrical, rigid-ligand systems showed the best performance.